THE FUTURE PHYSICS AT LEAR *

Rolf Landua

CERN – EP
and
University of Mainz, FRG

Abstract

The main physics motivation of the experiments proposed at LEAR in the post–ACOL phase is described: Test of fundamental symmetries (CP, T, CPT) and of QCD at low energies. Short technical descriptions of the experiments are given, with special emphasis on ambitious new techniques.

* Invited talk given at the Fermilab Low Energy Antiproton Facility Workshop, 10–12 April, 1986.

INTRODUCTION

The Low Energy Antiproton Ring (LEAR) at CERN is still the world's only high intensity source of low energy antiprotons. Since its commissioning in 1983, 16 experiments involving more than 300 physicists have taken data. Their motivations, experimental setups and their first results are summarized in these proceedings [1].

In September 1986, during a nine-month shutdown of the CERN antiproton complex, a new $\bar{p}$ source (ACOL) will be installed, eventually bringing a tenfold increase of the $\bar{p}$ production rate to 10^{12} $\bar{p}$/day. Simultaneously, several improvements will be made at LEAR, among them the installation of electron cooling.
The "post-ACOL" phase of LEAR starts in summer 1987. Experiments will profit from higher $\bar{p}$ intensities ($\leq 5 \cdot 10^6$ $\bar{p}$/sec), longer spill length ($\leq$ 3 h), smaller momentum spread ($\Delta p/p = 10^{-4}$), and continuously scannable momenta in the range 100 - 2000 MeV/c.

This article attempts to give an overview of the wide range of physics covered by the post-ACOL experimental programme. No reference is made to pre-ACOL experiments which will continue taking data in 1987 and 1988 (PS 170, PS 185), since they have been described in detail elsewhere [2,3].

The report is split into two parts.
Section 1 outlines the physics motivations of the experiments and confronts the questions raised by theory with the basic experimental principles employed to find an answer. The theoretical background is presented from a uniform point of view based on the author's belief in quarks and gluons and the assumption that QCD might be the theory of strong interaction also at low energies. Section 1 is subdivided into the four paragraphs *CP Violation, $\bar{N}N$ Annihilation, Spin Physics,* and *Tests of CPT Invariance.*
Section 2 presents some of the proposed experiments in more technical detail. Special emphasis is given to new developments and new frontiers faced by the experiments.

This contribution is based largely on the proposals and their addenda submitted to the PSC Committee at CERN. Table 1 lists the proposals approved by this Committee. Table 2 summarizes some important global aspects of the experiments, like location, beam time requests, and their estimated time scales.

Many of the presented topics overlap with other contributions to this workshop. The reader is refered to these articles for more detailed discussions.

1. OVERVIEW

This section outlines the main physics questions motivating the post-ACOL experiments at LEAR, and the basic principles of the experimental methods.

1.1 CP and T Violation in K^0 Decays

One of the oldest unsolved problems of particle physics is the **origin of CP violation.** The phenomenology of CP violating effects is usually parametrized by ε, describing the K^0 and $\bar{K}^0$ mass eigenstate mixing, and ε', connected to the isospin dependent K^0 decay amplitude. So far the only non-zero measure is the parameter $\varepsilon = 2.3 \cdot 10^{-3}$, derived from the observation of $K_L \to \pi\pi$ and $K_L \to \pi l \nu$ decays.

Many viable models of CP violation exist [4]. None seems particularly compelling, since the amount of CP violation is always introduced as a free parameter.

It could arise solely from a new CP violating "superweak" interaction allowing first order $\Delta S = 2$ transitions (S = strangeness) between K^0 and $\bar{K}^0$, resulting in a small mixture of the CP eigenstates K_1 and K_2. Observable effects are confined in this model to a non-vanishing non-diagonal term in the $K^0 - \bar{K}^0$ mass matrix, but there are - because of the weakness of the interaction - no significant effects on the K^0 decay amplitudes.

The "standard model", based on three quark generations and electroweak SU(2)xU(1) theory, "explains" the origin of CP violation by a single non-vanishing phase in the 3x3 Kobayashi- Maskawa matrix originating in the (arbitrary) Yukawa coupling of the quarks to the Higgs boson. This model predicts, like many others, a CP violating contribution in the K^0 decay amplitudes (ε'), in addition to the CP impurity of the K_L state (ε). The amount of CP violation should differ for different transitions: it is therefore possible to measure ε', which is essentially the ratio of the $I=2$ $K_S \to \pi\pi$ amplitude to the $I=0$ $K_S \to \pi\pi$ amplitude, from a simultaneous study of K_L and K_S decays into both charged and neutral pion pairs.

Because a non-zero value of ε' would demonstrate that CP violation is not confined to the mass matrix, a great deal of experimental effort is devoted to its measurement. The "standard method" compares the two pion decay rates of K_S and K_L produced by protons striking a production target. The main difficulties arise here from the measurement of the decay rate $K_L \to \pi^0\pi^0$ in the background of the CP-allowed decay $K_L \to 3\pi^0$ as well as the separation of coherent from incoherent regeneration. The sensitivity achieved by present experiments allows to establish an upper limit ($|\varepsilon'/\varepsilon| \leq 5 \cdot 10^{-3}$) but an increase in the experimental resolution by at least a factor of 3 is required to severely constrain the models. In particular, a non-zero value of ε' would rule out the "superweak" model. At present two new experiments are in progress (E731 at FERMILAB, NA31 at CERN) aiming at a reduction in the error on $|\varepsilon'/\varepsilon|$ to 10^{-3}.

The **CP violation experiment at LEAR** (P82) represents a completely different approach. It will measure the CP violation parameters in 2π, 3π and semileptonic de-

cays by making very accurate measurements of the proper−time distributions of the decays of tagged K^0 and $\bar{K}^0$ beams. The expected T violation in these decay processes will also be determined.

The CP symmetric source of the neutral kaon beams with known strangeness is $\bar{p}p$ annihilation at rest into the final states $K^-\pi^+K^0$ and $K^+\pi^-\bar{K}^0$ [5], occurring with a frequency of $4\cdot10^{-3}$ per annihilation. Owing to this low probability and the small amplitude of ε' ($< 10^{-5}$), a total of 10^{13} annihilations is needed to reach the necessary accuracy. The strangeness of the neutral kaon is tagged by the associated charged kaon, identified on−line in a magnetic spectrometer and a combined TOF−Cerenkov trigger. Neutral and charged decays of the kaons are detected in an electromagnetic calorimeter using lead converters and streamer tubes. The detector is described in more detail in section 2.1.

This approach allows to extract simultaneously the amplitudes (η_{+-}, η_{00}) and the phases (ϕ_{+-}, ϕ_{00}). The accuracy of $|\varepsilon'/\varepsilon|$ will be $2\cdot10^{-3}$. The final result will not be more precise than that of the K_S-K_L experiments carried out with proton beams, but it will be an independent measurement with very different experimental biasses. In addition, the method gives access to CP violation in the 3π channel (η_{+-0}, η_{000}).

A violation of T invariance has to accompany the clear violation of CP invariance, if our world is described exactly by a CPT invariant theory. Despite of the experimental limit of $6\cdot10^{-19}$ for CPT invariance [6] in the neutral kaon mass matrix, there is no *direct* experimental evidence for the violation of T invariance. The best existing test of T invariance is the limit $< 6\cdot10^{-25}$ e·cm on the electric dipole moment of the neutron [6]. This value is hardly compatible with most milliweak models of CP violation, but no final conclusion can be drawn at present.

A direct demonstration of T violation would be a difference in the transition rates $K^0 \to \bar{K}^0$ and $\bar{K}^0 \to K^0$, i.e. a failure of the principle of detailed balance. The experimental method used here originates from an idea of Kabir [7] and is the observation of the semileptonic decays of neutral kaons with well−defined initial strangeness.
A neutral kaon initially produced as a K^0 can change into a $\bar{K}^0$ at a later time, and similarly a $\bar{K}^0$ into a K^0. The strangeness of the neutral kaon at the time of its production is determined from the associated charged kaon. Its strangeness at the time of its decay is determined from the semileptonic decay using the $\Delta Q = \Delta S$ rule [6], i.e. $K^0 \to \pi^-e^+\nu$, $\bar{K}^0 \to \pi^+e^-\bar{\nu}$. The expected T violation would result in a time−independent rate asymmetry

$$a_T = \frac{R(K^0\to\bar{K}^0) - R(\bar{K}^0\to K^0)}{R(K^0\to\bar{K}^0) + R(\bar{K}^0\to K^0)} \approx 2\ \mathrm{Re}\ \langle K_L|K_S\rangle \approx 4\ \mathrm{Re}\ \varepsilon = 6.5\cdot10^{-3}$$

A small failure of the $\Delta Q = \Delta S$ rule would influence the detailed measurement in a highly recognizable way by a strongly enhanced asymmetry at early neutral kaon proper times $t \leq \tau_S$ (K_S lifetime). The measurement will therefore also bring a factor 10 improvement on the validity of the $\Delta Q = \Delta S$ rule. Table 3 compares the present accuracies of the CP and T violation parameters with the achievable accuracies of this experiment.

1.2 $\bar{N}N$ Annihilations

Today QCD seems to be the theory of strong interactions; a large number of its quantitative predictions have been verified experimentally. Unfortunately, the only true realm of QCD is the high energy[1] domain, which is $E \geq 3$ GeV in this context. Although more "precision" experiments with charmonium or bottomium states are necessary to improve QCD calculations for bound states of heavy quarks, the level of theoretical understanding already achieved here is considerable.

In contrast, our understanding of the long-distance dynamics of QCD, of the light hadron masses, and the confinement problem is still very poor [8]. Why do relativistic, strongly coupled bound states of quarks appear in just the configurations expected in a non-relativistic model with an instantaneous potential? Why do ideal mixing and the OIZ rule work to such a good approximation for light mesons, why do sum rules based on a short distance expansion provide a good description of the light meson spectrum? Does this unexpected success of simple ideas suggest an unexpected weakness of the "strong" interaction, in contrast to the commonly believed strong increase of the QCD parameter Λ at low energies?

A central issue of QCD is the self-coupling between gluons. This immediately leads to the prediction of bound states of two or three gluons ("glueballs": gg, ggg) or of $\bar{q}q$ states with a constituent gluon ("hybrids" : $\bar{q}qg$). But: where are they?

Calculations based on bag or flux tube models, QCD sum rules or lattice gauge theories agree that glueballs and hybrids should exist in the mass region between 0.7 and 3 GeV, but no agreement has yet been reached about their quantum numbers, width, and decay properties. Glueball candidates have been found ($E/\iota(1420)$,$\Theta(1720)$, $\xi(2220)$), but no final conclusion has yet been reached about their actual nature. The discussion, whether the $K\bar{K}\pi$ enhancement around 1420 MeV is a glueball or not demonstrates clearly that without a complete understanding of the spectrum of "normal" mesons it will not be possible to determine uniquely whether a given state is exotic or not. It is conceivable that exotic states appear with quantum numbers also accessible to normal mesons, and that the observed states are in fact mixtures of $\bar{q}q$ states with these exotics.

The experimental situation is unsatisfactory: only 3 out of the 6 ground state nonets ($L=0$, $L=1$), namely the 0^{-+}, 1^{--}, 2^{++} nonets, of the non-relativistic SU(3) $\bar{q}q$ model are complete. The other 3 nonets (1^{++}, 1^{+-}, 0^{++}) have doubtful (1^{+-}: H(1190); 1^{++}: E(1420)) or missing members (1^{+-}: H'). Two members of the scalar nonet, the δ and the S^*, are suspected to be $qq\bar{q}\bar{q}$ states. For the radially excited nonets, and for nonets where the $\bar{q}q$ pair has angular momentum $L \geq 2$, the situation is even less clear.

---

[1] The meaning of "high energy" varies with time and usually amounts to the maximum achievable center-of-mass energy in the world plus 10 %.

One of the most attractive ways to gain more insight into these questions is still the study of $\bar{p}p$ annihilation at low energies. Since the annihilation starts from an extended system of quarks and gluons, it allows the formation of exotic configurations even with quantum number not accessible by $q\bar{q}$ systems. The purely mesonic final state is a good starting point for meson spectroscopy, and partial wave analyses are much simpler with the absence of baryons in the final state.

Previous experiments suffered from several constraints. The bubble chamber technique implies very long measuring times and no possibility to select on-line specific final states, hence relatively low statistics. Counter experiments (e.g. ASTERIX) have overcome these obstacles, but substantial improvements such as better γ detection, momentum resolution and final state identification (π/K separation) are highly desirable.

What are the requirements for experiments to be performed to progress in the understanding of low energy QCD? Future experiments have to provide **high statistics, high resolution, exclusive measurements** of the initial and final state of $\bar{p}p$ (and eventually $\bar{N}N$) annihilation. They should give detailed data on resonances and their production and decay branching ratios, and data on total and differential cross sections for exclusive two-body annihilations in flight as a function of the initial state, energy, isospin and spin.

High statistics brings into view structures which cannot be seen in any other way, and exotic states seem to be rare. The possibility to **trigger** on specific final states is of great importance to select the channels of special interest. These can be channels either favoured by theory, or which could not yet be studied due to experimental limitations.

With **high resolution,** narrow resonances appear over a reduced background, and narrow intermediate states (e.g. π^0, η, η', ω, K_S) can be combined with other final state particles more unambiguously. Moreover, partial wave analyses of mass regions with encompassing resonances can be carried out in finer energy steps giving more insight into the resonating behaviour of the respective partial waves.

Exclusive measurements of the initial and final state of the annihilation allow to take advantage of conservation laws (J, P, C, I, G) to reduce the number of possible intermediate states. The initial state selection for $\bar{p}p$ annihilation at rest proceeds via the choice of a liquid target (mainly s wave annihilation) or a H_2 gas target using a trigger on L X-rays which indicates p wave annihilation. This technique has been demonstrated successfully in the ASTERIX experiment at LEAR.
A complete reconstruction of the final state requires the detection and identification of charged and neutral particles, i.e. pions, kaons and gammas, over the complete solid angle and over the full momentum range.

The following section describes the experiments proposed at LEAR, and how their experimental setup will attempt to match the requirements mentioned above.

Two experiments *(Crystal Barrel, OBELIX)* will study $\bar{N}N$ annihilations at rest and in flight using an extracted $\bar{p}$ beam. They agree in their main physics objectives:

- Normal meson spectroscopy
- Search for exotic states (glueballs, hybrids, $qq\bar{q}\bar{q}$ states)
- Study of $\bar{p}p$ annihilation dynamics at rest and in flight

Although they have common features in the experimental set-up, they have specific differences which make them complementary in the study of the annihilation process.

The common features are:

- magnetic spectrometers surrounded by electromagnetic calorimeters
- approximate 4π geometry for the detection of charged and neutral particles
- exchangeable liquid and gaseous H_2 targets to select the initial atomic state (s- or p-wave) of the annihilation
- comparable momentum resolution for charged particles (σ = 2.8 % at 1 GeV/c)

The main differences are in the gamma energy resolution, the separation of charged pions and kaons, and in the trigger possibilities for neutral final states and charged kaons. In addition, one experiment (OBELIX) will have a charge-exchange target in front of the detector providing a source of antineutrons to study also $\bar{n}$ annihilations at very low energies.

The **Crystal Barrel (P90)** detector design comprises an electromagnetic calorimeter (16 X_0 of CsI) providing an excellent energy resolution σ = 2% at E = 1 GeV. The main emphasis will therefore be put on the investigation of annihilation channels containing more than one neutral particle in the final state, e.g. $\pi^0\pi^0$, $\eta\eta$, $\eta\eta'$. Resonances decaying via $\pi^0\pi^0$ or $\eta\eta$ are pure I=0 states (like glueballs), and copious background sources as the ρ (I=1) will not be contained in the same final state. Some annihilation channels are only accessible with at least two neutrals in the final state (e.g. $\bar{p}p \rightarrow \pi^0\omega$). Only few data exist here because of the limitations in the γ detection of previous detectors. The gamma energy resolution will allow to reconstruct π^0 or η mesons online and use this information for trigger purposes. For more details see section 2.2.1.

The **OBELIX (P95)** detector is based on the Open Axial Field Spectrometer from the ISR with the addition of a position sensitive electromagnetic calorimeter with high angular resolution (σ = 2 mrad) (proportional drift tubes, limited streamer tubes from the CHARM I experiment). The single γ energy resolution, normally σ = 18 % at 1 GeV, improves considerably to σ = 2.5 % at 1 GeV requiring the conversion $\gamma \rightarrow e^+e^-$ in the inner TOF scintillator and measuring the e^+, e^- momenta. A particular feature is the charged π/K separation up to 1 GeV/c by TOF, also allowing to trigger on charged kaons in the momentum band 200 - 600 MeV/c.

The main emphasis will be put on final states containing kaons, since the statistics on these final states is limited due to the lack of an efficient trigger in previous experiments and the rareness of these final states (about 7 % of all $\bar{p}p$ annihilations). In addition, it is often conjectured that glueballs might decay flavour-blind, or even couple more strongly to $s\bar{s}$ than to $u\bar{u}$ or $d\bar{d}$ states: a small signal from glueballs decaying into kaonic final states would then appear over a much reduced background, and hence be easier to observe. For more details see section 2.2.2. A comparison of the Crystal Barrel and OBELIX detectors with previous detectors is given in Table 4.

A different approach are experiments *inside* the LEAR ring. With an **internal hydrogen gas jet target** the small momentum spread of the LEAR beam translates directly into a very good energy resolution ($\Delta \sqrt{s} \leq 1$ MeV). The study of $\bar{p}p$ annihilation while scanning the center of mass energy region 1.9 – 2.4 GeV in small steps, together with the achievable high luminosities, can give access to narrow and rare new resonances. Moreover, polarized atomic hydrogen jet beams allow the study of the spin-dependence of exclusive annihilation reactions.

In this way, the **JETSET (P97)** experiment will study the two-body annihilations

$$\bar{p}p \rightarrow \Phi\Phi \rightarrow K^+K^-K^+K^-$$
$$\bar{p}p \rightarrow K_S K_S \rightarrow \pi^+\pi^-\pi^+\pi^-$$

i.e. the differential cross-section and the polarization parameter P in the energy range 1.9 – 2.4 GeV using an internal gas jet target. The process $\bar{p}p \rightarrow \Phi\Phi$ attracts much attention because of its purely gluonic intermediate state. Possible quantum numbers of this state are 0^{-+}, 0^{++}, 1^{++}, 2^{++}, 2^{-+}, ... with I = 0. In the proposed first phase, the JETSET detector will have no magnetic field. It will comprise an inner tracking system based on Si microstrip and straw chambers to identify and to measure charged tracks. The online π/K identification within 1 μsec will rely on a fast Cerenkov RICH counter, while an outer layer of trigger scintillators will give information about the multiplicity of an event.
For more details and a possible upgrading of the detector see section 2.2.3.

1.3 Spin Physics

The spin dependence of the $\bar{N}N$ interaction reflects the underlying structure of the interaction between quarks and gluons confined inside a nucleon.

Microscopic calculations based on the quark−gluon picture have recently gained importance, but the intrinsic difficulties of non−perturbative QCD calculations force most theoretical approaches to start from potential models based on meson exchange [9]. This picture is probably appropriate for the medium and long range part of the real potential V, but for $r < 0.8 - 1$ fm, the quark bags making up the nucleon and antinucleon start to overlap appreciably, and the representation of V as a local meson exchange potential breaks down. It is therefore not clear if the success of including vector meson exchange (ρ,ω) into the short−range NN theory is accidental and does in fact parametrize a different process such as quark or gluon exchange between two overlapping bags.

Many experimental data are available to allow a good phenomenological description of the NN potential. In the meson exchange picture, the real part of the $\bar{N}N$ potential is obtained from the NN potential by a G parity transformation. The usefulness of this approximation is again limited to medium and long ranges, since the short−range part is generally treated phenomenologically, and there are no clear prescriptions how to transform it from the NN to the $\bar{N}N$ case. Moreover, large cancellations occur between the scalar (ε) and vector (ω) meson contributions to the NN central potential, which are absent in the $\bar{N}N$ case. Finally, the annihilation of $\bar{N}N$ into mesons has no NN counterpart, and the effective complex annihilation potential is unknown.

What are possible experimental paths to improve our knowledge about these fundamental questions? Information can come from:

1. Measurements of the spin−dependent differential cross section for elastic scattering $\bar{p}p \rightarrow \bar{p}p$ over the whole low energy range. A complete phase shift analysis will be more sensitive to resonance effects in the elastic channel through spin−dependent observables.

2. Measurements of the spin−dependent differential cross section for $\bar{p}p$ annihilation. These will reveal any inelastic coupling of s−channel resonances; 2−body final states like $\pi\pi$ or KK are sensitive filters for specific quantum numbers. Here, only 1^{--}, 2^{++}, 3^{--}, ... partial waves contribute and make the partial wave analysis much simpler. There is hope that this method provides in particular access to broad structures, which are notoriously difficult to extract from total cross sections [10].

The experimental access to information about the $\bar{N}N$ spin dependence is very difficult but needed to obtain a better theoretical understanding. At low energies, only few crude data exist on the $\bar{p}p$ elastic polarization. The analysis of results from $\bar{p}p$ elastic scattering, although the simplest from an experimentalist's point of view, is very complex: four spin−1/2 particles in two possible isospin states are described by

five helicity amplitudes for each isospin [11]. This complexity does not allow a complete phase shift analysis without the knowledge about initial and final spin configurations. The use of a polarized beam and a polarized target would change the situation considerably. Unfortunately, the analyzing power of carbon for $\bar{p}$'s [12] is too small to produce a polarized $\bar{p}$ beam by scattering off carbon or to use carbon as the polarization analyser for $\bar{p}$'s, thus depriving the experimentalists of two essential tools which were extensively used to measure spin-dependent observables in the NN system.

Different experimental approaches are therefore needed and several methods have been proposed, which will be discussed in the following.

A method to **polarize $\bar{p}$'s circulating inside LEAR** has been proposed (P92) and the technique will be tested with protons in a "Test Storage Ring" (TSR) currently under construction in Heidelberg. The main idea is to install a **polarized atomic hydrogen gas target** inside LEAR and to use the spin-dependent strong interaction to filter out preferentially one of the two possible spin states of the circulating $\bar{p}$'s. However, the singlet- and triplet- elastic scattering cross-sections - unknown at present - must differ sufficiently to permit a useful builtup of polarization before the competing annihilation process, with about twice the cross-section of elastic scattering, leads to a serious decrease of the beam intensity [13].

The best area density of an ordinary polarized atomic hydrogen beam is about 10^{12} $\vec{H}/cm^2$, which is insufficient to polarize the LEAR beam within a reasonable time (e.g. 10 h). In order to increase the target density an intense $\vec{H}$ atomic beam will be injected into a thin-walled storage cell where the density on the beam axis is expected to be about 10^{14} $\vec{H}/cm^2$.

The test measurements in the TSR have to demonstrate two important results before the method can be employed at LEAR:

- The polarization lifetime of protons circulating in a storage ring similar to LEAR is long enough to apply the filter method in this energy range.
- The integration of a high density internal gas target and a detector system for charged particles into a UHV system ($p = 10^{-12}$ Torr) is possible.

In case of success, the experiment will use the internal target both as a polarizing **and** a reaction target. The efficiency of this method would surpass a normal double scattering experiment by several orders of magnitude and would allow the measurement of up to six spin correlation coefficients in the $\bar{p}p$ elastic and the charge exchange scattering.
A different method to separate the two spin components of the circulating $\bar{p}$ beam spatially by a magnetic gradient field has been proposed and is presently under consideration at CERN. The principle of the method is described in these proceedings [14].

Since polarized $\bar{p}$ beams will not be available in the next few years, the only means to explore spin-dependent effects is the use of a **polarized target.**

The **study of spin-dependent observables in elastic $\bar{p}p$ scattering** (P91) will use a frozen spin target and a high resolution spectrometer (SPES II) to measure the polarization $P(\theta)$ and the polarization transfer parameter D over the momentum range 300 – 700 MeV/c. A recoil proton polarimeter together with the spin rotation facility provided by the magnetic field of the SPES II spectrometer will allow a more complete measurement of the polarization components in the scattering plane.

The **measurement of the spin-structure of the reaction $\bar{p}p \rightarrow \bar{n}n$** (P93) will allow to extract the same parameters P and D for the charge-exchange reaction at various momenta between 300 – 2000 MeV/c over a large angular range, using a polarized (frozen-spin) target. Several theoretical predictions agree that long-range tensor forces acting coherently should induce large effects on the spin observables in the charge-exchange reaction, so that almost completely polarized $\bar{n}$'s might be produced [15]. In addition, the charge exchange process is a very clean one in the meson exchange picture, since only π and ρ appear in the t channel, and it might be sensitive to the presence of small resonating amplitudes.

1.4 Tests of CPT Invariance

The CPT theorem states the invariance of fundamental physical laws under the combined symmetry transformations C,P and T. The derivation starts from very general assumptions: rotational and Lorentz invariance, microcausality and spin-statistics connection. Particular predictions are the identity of mass, magnetic moment and decay width of particles and antiparticles, except for a reversal of the sign of the magnetic moment.

No experimental evidence for a CPT violation has yet been found. The most sensitive test arises from the very small $K_S - K_L$ mass difference which allows to conclude that the mass eigenvalues of the K^0 and $\bar{K}^0$ eigenstates must differ by less than $6 \cdot 10^{-19}$ [6].

However, the fundamental importance of CPT invariance demands experimental verification under various circumstances with the highest achievable precision. At LEAR, four experiments have been proposed: two experiments to compare the inertial mass of proton and antiproton, one experiment to measure the $\bar{p}$ gravitational mass, and one experiment aiming at the production of antihydrogen for later use in $\bar{H}$ spectroscopy.

The **high precision determination of the $\bar{p}-p$ inertial mass ratio** is motivated by the fact that the best limit for CPT invariance in baryonic systems comes from the $\Lambda - \bar{\Lambda}$ mass difference ($7 \cdot 10^{-6}$) [6], and an achievable accuracy of 10^{-9} could improve this limit by four orders of magnitude. Since it is not clear how a violation of CPT would affect masses, it is conceivable that a three-quark system is affected differently than a quark-antiquark state.
Both experiments will compare the cyclotron frequency ν_c of antiprotons and protons (or H^- ions) orbiting in a very homogeneous magnetic field.

In the **RF mass spectrometer (P52),** $\bar{p}$ or H^- ions of approximately 100 keV kinetic energy will circulate in a magnet of 1 m diameter. The natural linewidth of the cyclotron resonance curve is expected to be $10^{-6}\ \nu_c$, requiring a 10^{-3} accuracy in the determination of the peak centroid to reach the precision of 10^{-9}.

The other approach starts from ultra-low energy (milli-eV) antiprotons confined in a **Penning trap (P83).** Previous measurements of the proton mass with the same method have demonstrated an achievable natural linewidth of $10^{-9}\ \nu_c$. However, the technique of trapping and cooling $\bar{p}$'s to milli-eV energies has yet to be developed.
A more detailed description of the intrinsic difficulties of both methods is given in section 2.3.

The **gravitational mass of the antiproton (P94)** is unknown from an experimental point of view. The CPT theorem assumes flat space-time, and it is not obvious that it will also hold in gravitational fields, i.e. curved space-time, so it cannot be invoked to argue that antimatter also obeys the equivalence principle.
Moreover, in certain models of supergravity, the graviton has a vector partner, the "gravi-photon" [16]. This additional vector interaction would repel matter but attract antimatter to the earth [17]. If the gravi-photon were massive, the additional interaction would be of finite range and no observable astrophysical consequences would result. Presently, experiments [18] leave room for such a component in the earth's gravitational field with a range between 5 m and 10 km and a relative strength of 10^{-2} or less.
Recent geophysical measurements [19] of the gravitational constant G have revealed systematic discrepancies with the value of G as measured by Cavendish type experiments in the laboratory. They could be interpreted as evidence for the real existence of such a component.

The measurement of the $\bar{p}$ gravitational acceleration will also start from ultra-low energy antiprotons stored in a Penning trap, which are then launched vertically up a drift tube. The time of-flight up the drift tube, which protects the antiprotons from external electromagnetic stray fields, together with the initial velocity gives a measure of the gravitational force acting on the particles. The TOF distribution of antiprotons will be directly compared with the distribution for H^- ions.
The energy loss of the particles rising 1 m in the gravitational field, $\Delta E = m \cdot g \cdot \Delta h = 10^{-7}$ eV, is very small compared to the average thermal energy of $\bar{p}$'s stored in the trap. Hence only particles situated in the very low energy tail of the Boltzmann distribution will be sensitive to gravitational effects. Many repetitive measurements of the end of the drifttime distribution have to be made to accumulate enough statistics to determine precisely the "cut-off" region. Particles arriving at the "cut-off time" have used up all their initial energy, slower particles will fall back to the trap.
The intended precision of 1 % will be reached by launching $10^6 - 10^7$ antiprotons, and comparing the distribution with the distribution for H^- ions. For more details on the main difficulties of the experiment see section 2.3.3.

The availability of **antihydrogen atoms** would enable experimentalists to repeat the precision measurements done with hydrogen atoms (Rydberg constant, hyperfine structure, Lamb shift). But, at present, not even a single antihydrogen atom has been produced. Therefore it has been proposed to study the **feasibility of $\bar{H}$ formation (P86)** by radiative capture of positrons by antiprotons in LEAR.
The spontaneous $\bar{H}$ formation rate would be small: 1 / (15 min), assuming available e^+ "beam" intensities of 1 cm^{-3} (with a Na−22 source of 10 Ci) and 10^{10} $\bar{p}$'s in LEAR. The theory predicts an enhancement by laser−induced recombination. The gain factor can be measured by inducing recombination of protons circulating in LEAR and co−moving electrons from the electron cooling device. It is proposed to mount two spherical mirrors at both ends of the straight section SL3 to let an injected laser beam interact several times with the $p-e^-$ beams. Theoretical calculations [20] predict a gain factor of 100 for a laser pulse intensity of 20 MW/cm^2 and a laser wavelength resonant with the transition from the continuum to the $n=2$ state of hydrogen.

Improvements of several orders of magnitude will be needed to reach a $\bar{H}$ formation rate useful for spectroscopic experiments. However, these factors might be achievable by more intense e^+ and $\bar{p}$ beams.

Different methods for the production of antihydrogen, e.g. starting from antiprotons stored in a Penning trap, have been proposed at this conference [21].

2. EXPERIMENTAL AIMS AND TECHNIQUES

2.1 CP and T Violation in K^0 Decays (P82)

The study of about $4 \cdot 10^9$ neutral kaon decays into $\pi^+\pi^-$ or $\pi^0\pi^0$ produced in 10^{13} $\bar{p}$ annihilations at rest will be needed to reach the required accuracy in the determination of ε'/ε ($2 \cdot 10^{-3}$). 90 % of the data will be analysed on line, and only 10 % – comprising all 3π and semi-leptonic decays – will be written on tape and analysed off-line ($\approx$ 5500 h CPU time, IBM-3081 equivalent).

Therefore the detector must be suited for:

- online identification of $K^-\pi^+K^0$ and $K^+\pi^-\bar{K}^0$ events (i.e. charged kaon identification, $K^{\pm}\pi^{\mp}$ missing mass calculation)
- online reconstruction of the K^0, $\bar{K}^0$ decay products and the decay vertex for $K^0, \bar{K}^0 \to \pi^+\pi^-$ and $K^0, \bar{K}^0 \to \pi^0\pi^0$
- offline reconstruction of $K^0, \bar{K}^0 \to \pi^+\pi^-\pi^0$, $3\pi^0$, $\pi l\nu$

Fig. 1 shows a cross-section through the proposed detector. It is a magnetic spectrometer with cylindrical symmetry based on the DM2 spectrometer constructed at Orsay. It is equipped with an inner multiwire proportional chamber, 6 drift chambers, a system of TOF scintillators and Cerenkov counters to identify charged kaons, and an electromagnetic calorimeter with good position resolution inside the magnet coil to measure the position and direction of the π^0 decay gammas.

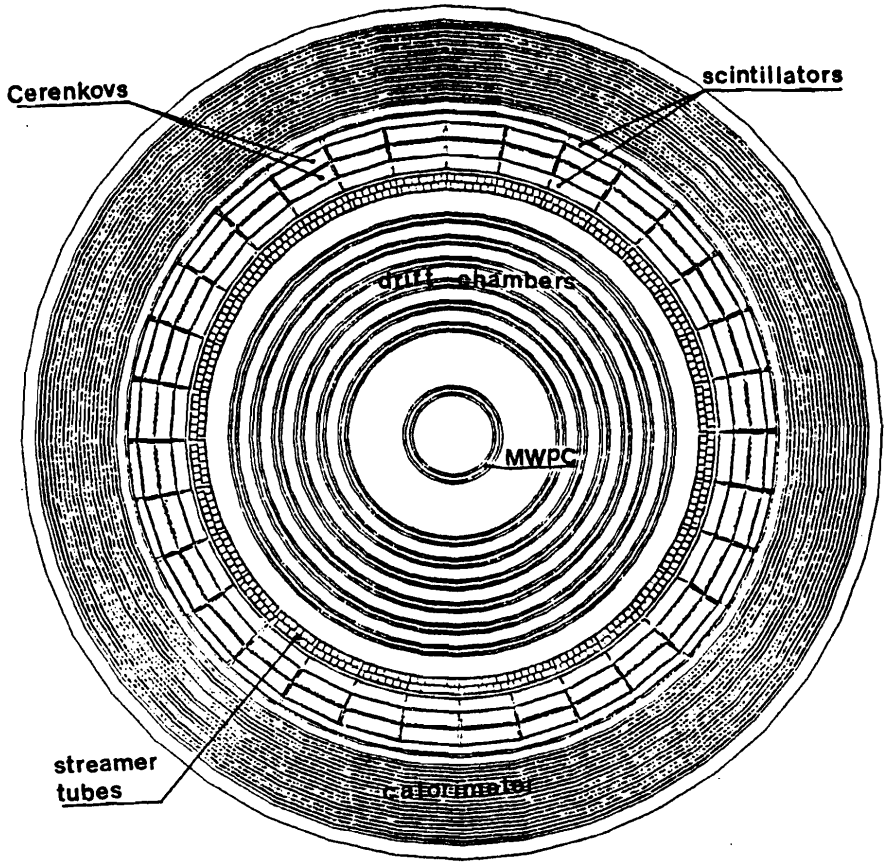

Fig. 1 Cross-section of the proposed detector to study CP and T violation at LEAR

The $K^{\pm}\pi^{\mp}$ pair will be tracked on-line by two hardware processors giving the missing mass with 60 MeV resolution within 1 μsec. The K^0 decay products will be identified in the drift chambers and the electromagnetic calorimeter. A third processor combines these informations within 250 μsec to reconstruct the event topology completely.

Measurements of the asymmetries – integral and differential – of K^0 and $\bar{K}^0$ decays will be performed. Asymmetries in the $\pi^+\pi^-$ and $\pi^0\pi^0$ decays will be used to measure *simultaneously* the two-pion decay amplitudes and phases η_{+-}, ϕ_{+-}, η_{00}, and ϕ_{00}. For example, the time-dependent asymmetry $A_{+-}(t)$ of the $\pi^+\pi^-$ decay mode is:

$$A_{+-}(t) = \frac{R(\bar{K}^0 \to \pi^+\pi^-) - R(K^0 \to \pi^+\pi^-)}{R(\bar{K}^0 \to \pi^+\pi^-) + R(K^0 \to \pi^+\pi^-)}(t) = 2\left[\frac{|\eta_{+-}| e^{\frac{1}{2}\gamma_S t} \cos(\Delta m \cdot t - \varphi_{+-})}{1 + |\eta_{+-}|^2 e^{\gamma_S t}} - \mathrm{Re}\,\varepsilon\right]$$

The function $A_{+-}(t)$ is plotted in Fig. 2.

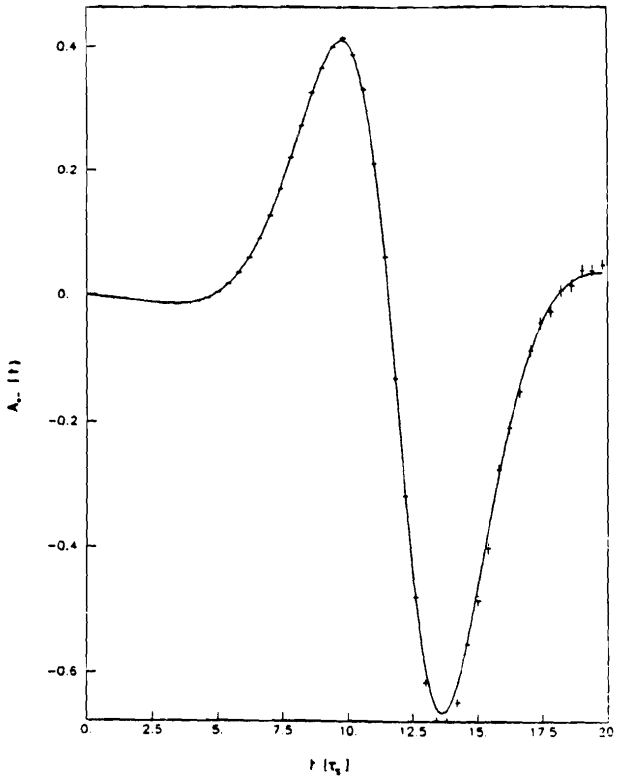

Fig. 2 **Expected decay rate asymmetry $A_{+-}(t)$ as a function of the neutral kaon eigentime**

The accurate determination of the kaon decay eigentime is connected to the precision of the vertex determination. For $\pi^+\pi^-$ a precision $\sigma = 2$ mm will be achieved, while the $\pi^0\pi^0$ vertex determination depends critically on the spatial resolution of the calorimeter. With the actual design, a resolution $\sigma = 1.6$ cm for $\pi^0\pi^0$ and $\sigma = 6.1$ cm for $3\pi^0$ decays can be achieved.

The final accuracies obtainable with 10^{13} $\bar{p}$ annihilations in the target are given in table 3.

2.2 $\bar{N}N$ Annihilation

2.2.1 Crystal Barrel (P90)

The Crystal Barrel detector (Fig. 3) is a magnetic spectrometer with cylindrical geometry, covering a large solid angle, and with a high energy resolution electromagnetic calorimeter. It will be used to study $\bar{p}p$ and $\bar{p}n$ annihilation at rest and in flight ($p = 100 - 2000$ MeV/c), with specific emphasis on:

- Search of glueballs and hybrids, in particular in final states with several neutrals
- Study of radiative and rare meson decays
- Study of $\bar{p}p$ annihilation dynamics from initial atomic s− and p−states
- Search for $\bar{p}p$ bound states
- Phase−shift analyses of exclusive two−body annihilation reactions as a function of energy

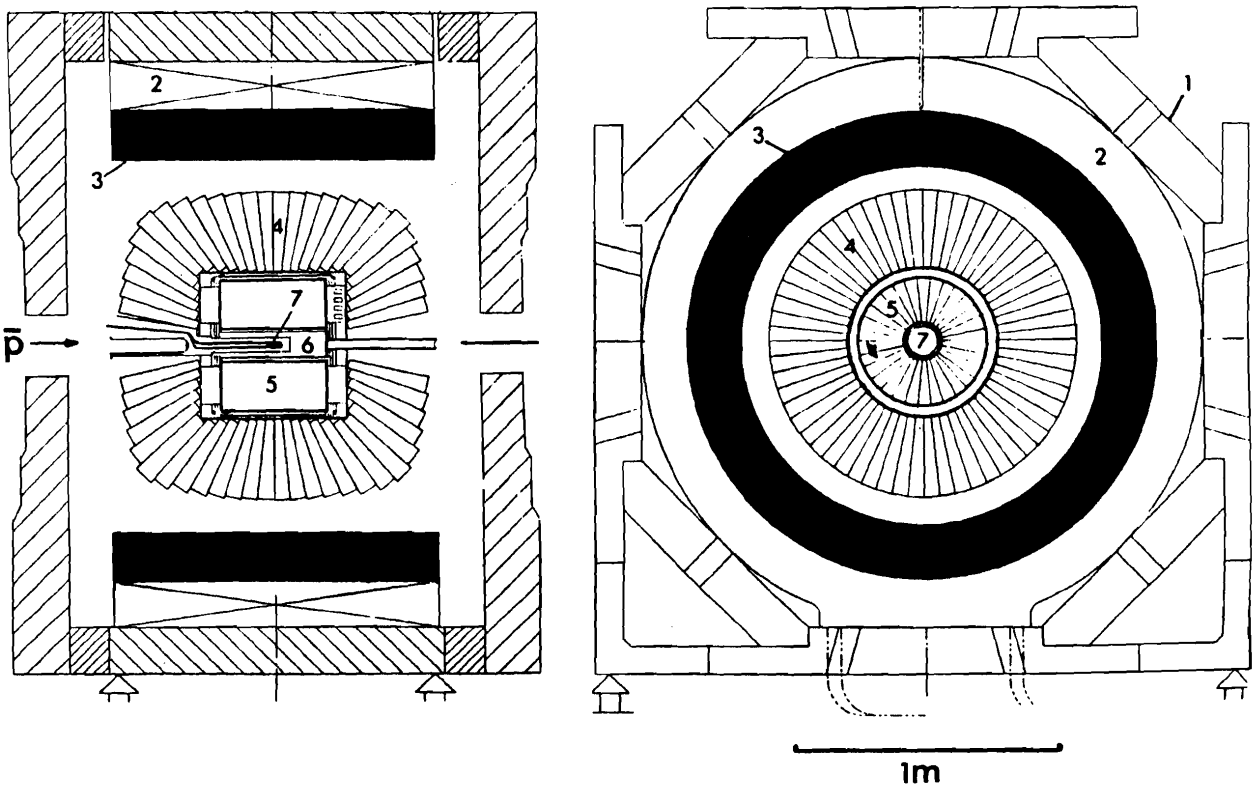

Fig. 3 CB Apparatus: (1) Yoke (2) Old Coil (3) New Coil (4) CsI Barrel (5) JDC (6) XDC/PWC (7) LH_2 target

The *magnet* will be an upgraded version of the DM1 magnet previously used in the ASTERIX experiment. The maximum field strength will be 1.5 T, with an homogeneity of $\leq$ 2 % over the spectrometer.

Two exchangeable combinations of *target and central detector* are foreseen:

- Liquid H_2 [s wave annihilation] surrounded by two cylindrical multiwire proportional chambers to trigger on the final state multiplicity or a $K_S \rightarrow \pi^+\pi^-$ decay
- H_2 gas target at NTP surrounded by an X-Ray Drift Chamber (XDC) [22] to trigger on L X-rays [p wave annihilation] and to image charged tracks close to the annihilation vertex

Charged particles are tracked within a solid angle of 99 % 4π. The average multiplicity in $\bar{p}p$ annihilations at these energies is 3.5 - 4. Their momentum is determined in the cylindrical Jet Drift Chamber (JDC). The design values are: 30 segments in ϕ (12^0), 32 radial samplings, measured track length 18.6 cm, spatial resolution σ = 100 μm using a "cool" gas with low drift velocities, flash-ADC readout, z position by charge division. A momentum resolution of σ = 2.8 % at 1 GeV/c is expected over a solid angle of 63 % 4π. The dE/dx resolution (σ = 10 %) will allow π/K separation up to 500 MeV/c.

The γ *detector* will comprise 1380 CsI crystals (16 X_0) with photodiode readout. The design values are: energy resolution σ = 2 % at 1 GeV over 95 % 4π, position resolution σ = 20 mrad above 200 MeV.

The *final state selection* proceeds by a multi-level trigger scheme. For example, L X-Ray and K_S candidates will be found within less then 3 μsec. The invariant mass of neutrals decaying into gammas will be calculated within 250 μsec.

2.2.2 OBELIX (P95)

The OBELIX detector (Fig. 4) is based on the Open Axial Field Spectrometer used at the ISR [23]. It is a large solid angle magnetic spectrometer with very good charged particle identification by dE/dx and TOF and with a high angular resolution gamma detector. It will be used to study $\bar{p}p$, $\bar{p}n$ and $\bar{p}A$ annihilations at rest and in flight (p = 100 − 2000 MeV/c), and the annihilation of antineutrons produced in a charge−exchange target in front of the detector. Special emphasis is given to:

- Search for glueballs, hybrids, and 4−quark states, especially in final states containing kaons
- Meson spectroscopy
- Study of $\bar{N}N$ annihilation dynamics as a function of the initial angular momentum, isospin and energy
- Search for quark−gluon aspects of nuclear matter

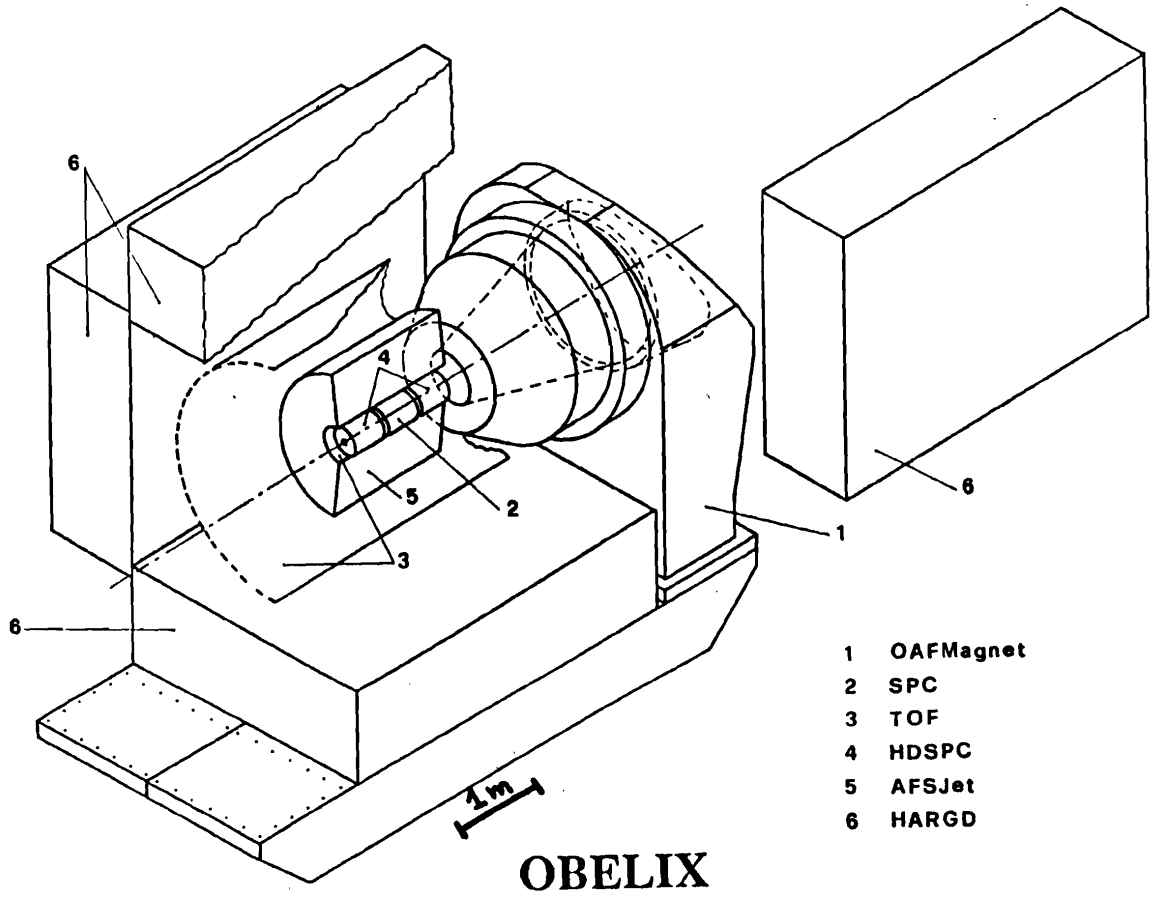

Fig. 4 Schematic view of the OBELIX detector

The *Axial Field Magnet* provides a magnetic field with axial symmetry and a central value of 0.5 T.

The *H_2 gas target* is surrounded by the *Spiral Projection Chamber (SPC)* [24] to provide a fast trigger on L X−rays [p wave annihilation] and to image tracks very close to the annihilation vertex, in particular spectator protons or nuclei from $\bar{p}d$ or $\bar{p}A$ annihilations. The target components can be quickly exchanged, e.g. with a liquid H_2 target.

Charged particles are tracked within a solid angle of 99 % 4π. Their momentum is determined in the AFS Drift Chamber, which has 82 segments in ϕ (4^0), 42 radial samplings, measured track length 60 cm, spatial resolution σ = 200 μm, ADC−TDC readout, charge division. The momentum resolution as measured at the ISR is σ = 2.7 % at 1 GeV over a solid angle of 75 % 4π.

The *TOF system* comprises two scintillator barrels at r = 18 and 135 cm, covering 75 % 4π. It allows to trigger on charged kaons in the momentum band 200 − 600 MeV/c, the detection of $\bar{n}$ annihilation, and an offline π/K separation up to 1 GeV/c.

The γ *detector* samples showers in 3 dimensions and consists of two main components: four large supermodules (4 x 3 x 1.1) m^3 built with lead converter foils and active elements [11,000 proportional drift tubes and 14,000 limited streamer tubes] used previously in the CHARM I experiment, and two cylindrical high density projection chambers of new design [25] in the endcaps. It covers 82 % 4π with a depth of 10 X_0. The position resolution is σ = 2 mrad and the energy resolution is σ = 18% at 1 GeV above 200 MeV. The energy of converted γ's ($\gamma \rightarrow e^+e^-$) is measured with a resolution σ = 2.5 % at 1 GeV.

The *final state selection* is based on a multi−level trigger scheme. Charged and neutral multiplicity and L X−ray candidates will be known within 3 μsec, and charged kaons will be identified in less than 100 μsec.

2.2.3 JETSET (P97)

The JETSET detector is a non−magnetic device to track charged particles and for π/K separation. It will surround an internal H_2 gas jet target in LEAR. The specific objectives of the experiment are to measure the differential cross section $d\sigma/d\Omega$ and the polarization parameter P in the reactions

$$\bar{p}p \rightarrow \Phi\Phi \rightarrow K^+K^-K^+K^-$$
$$\bar{p}p \rightarrow K_sK_s \rightarrow \pi^+\pi^-\pi^+\pi^-$$

at 12 different energies, giving access to interesting intermediate gluonic states.

The design of the *internal hydrogen gas jet target* is based on the experience gained in the ISR experiment R704 [26]. The target density will be $8 \cdot 10^{13}$ atoms/cm^2 resulting in a luminosity of $2.5 \cdot 10^{30}$ cm^{-2}s^{-1} for 10^{10} $\bar{p}$'s circulating in LEAR. A polarized atomic hydrogen beam can be obtained [27] by means of a Stern−Gerlach type separation in a sextupole magnet focussing only states with a certain spin orientation. The nuclear spin orientation is selected through RF transitions between hyperfine states. The target density for the polarized beam will be $1.5 \cdot 10^{12}$ atoms/cm^2, which is sufficient for experiments but has no polarizing effect on the LEAR beam.

A *fast ring−imaging Cerenkov counter (RICH)* has been designed [28] for π/K separation within 1 μsec or less. High speed is expected from a much faster TPC gas, and the trigger decision will be based on the different number of photoelectrons (1−2 below threshold, 20 above threshold) produced by kaons below threshold (threshold π: 180 MeV/c, K: 620 MeV/c).

The *tracking device* is a combination of Si microstrip detector [29] and straw vertex chambers developed at SLAC [30]. The microstrip system will provide 3 − 6 points per track along 10 − 20 cm with a precision of σ = 10 μm. The straw chamber system − 850 self−supporting aluminized mylar straws of 7 mm diameter and $5 \cdot 10^{-4}$ wall thickness − gives fast track finding capability and an accuracy of σ = 100 μm (transverse) and σ = 2 mm (longitudinal).

The collaboration intends an upgrade to a general purpose "phase 2" magnetic detector for charged and neutral particle spectroscopy. The plan is to add a superconducting solenoid (6 T) and an electromagnetic calorimeter with fine granularity (BGO crystals, energy resolution σ = 3 % at 1 GeV, position resolution σ = 7 mrad). Fig. 5 shows a cross−section of the experiment including the electromagnetic calorimeter and the superconducting magnet of the phase 2 detector.

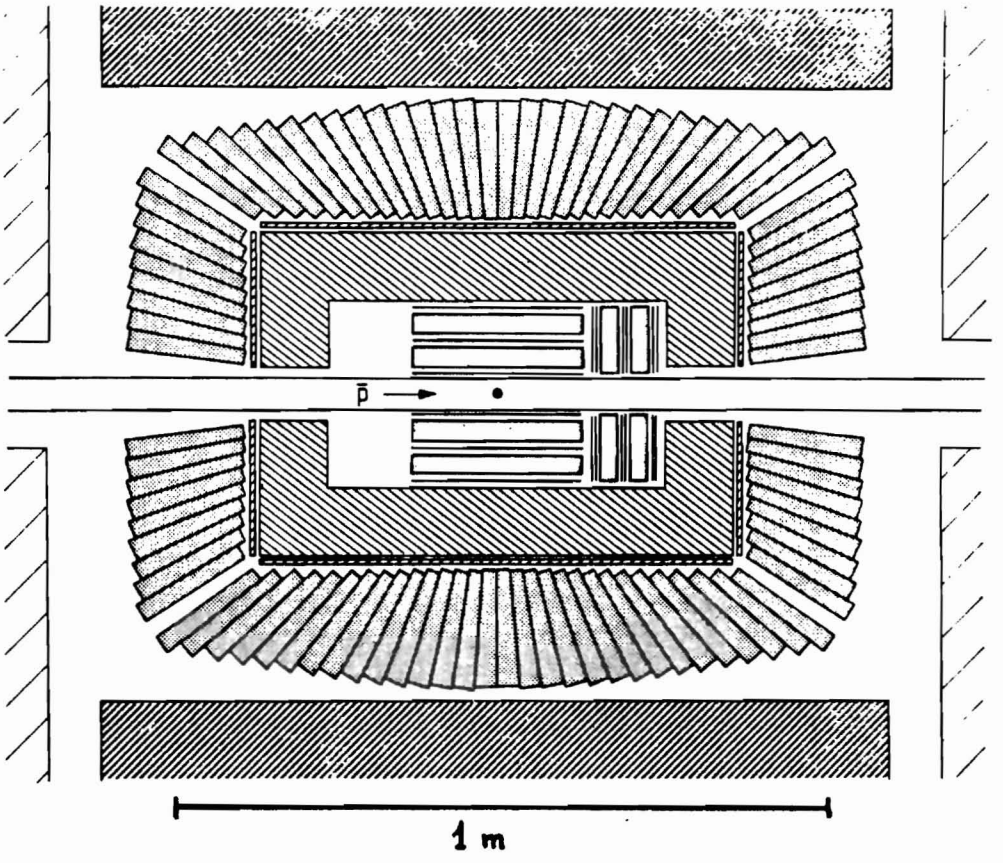

GAS JET (direction into paper)

SILICON MICRO-STRIP TRACKER (barrel: 3 z layers; end-cap: 3 x+y layers)

STRAW CHAMBER (barrel: 8 z layers; end-cap: 4 x+y layers)

FAST RICH (liquid C_6F_{14} radiator)

BGO ELECTROMAGNETIC CALORIMETER (photodiode readout)

SUPERCONDUCTING SOLENOID (6 Tesla)

FLUX RETURN (restricted to top and bottom sides of detector)

TRIGGER SCINTILLATION COUNTERS

Fig. 5 Cross – section of the JETSET "phase 2" detector
(including upgrade with superconducting magnet and BGO calorimeter)

2.3 $\bar{p}$ mass

2.3.1 Cold $\bar{p}$ Source

The technique of decelerating, trapping and cooling antiprotons in a Penning trap will be needed for two experiments (P83, P94) aiming at a measurement of the inertial and gravitational $\bar{p}$ mass. Since a cold $\bar{p}$ source with 10^7 $\bar{p}$'s stored at milli–eV energies has many possible applications, a short technical description of a Penning trap and of the $\bar{p}$ transfer scheme follows.

The *Penning trap* consists of two endcap electrodes and one ring electrode with cylindrical symmetry and hyperbolic surfaces (see Fig. 6). The electric field produced by this configuration, when properly biassed – i.e. negative endcaps, positive ring – will confine a $\bar{p}$ along the vertical axis, but will repel it towards the ring electrode in the horizontal plane. A magnetic field parallel to the vertical axis will force any transverse motion into a cyclotron orbit with a superimposed E x B magnetron drift. Fig. 7 shows the resulting motion of a confined particle inside the trap.

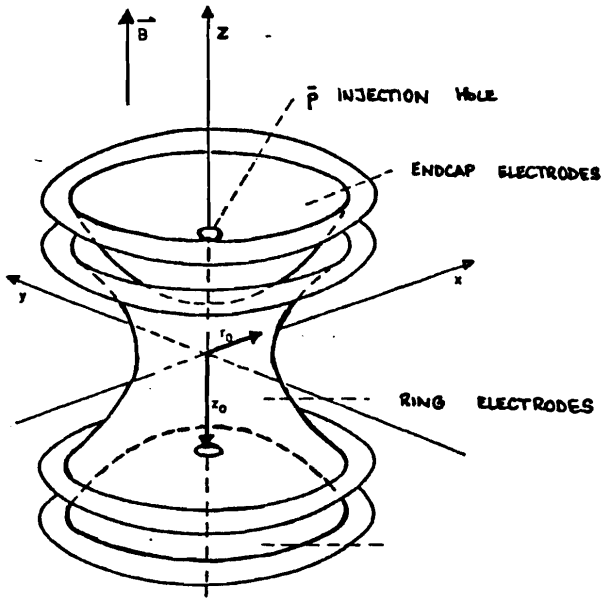

Fig. 6 Schematic view of a Penning trap

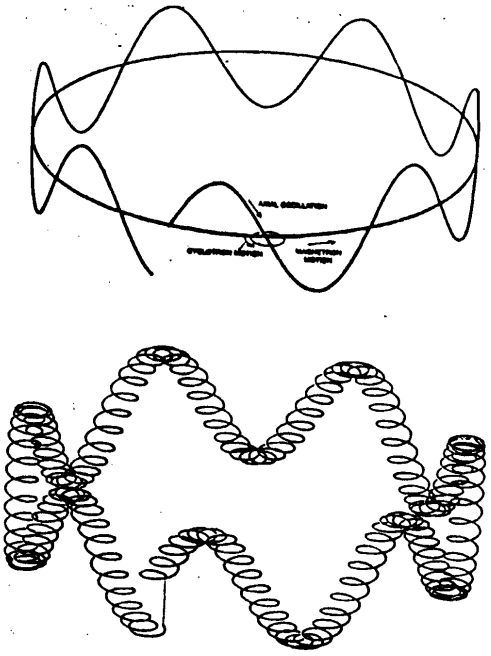

Fig. 7 Motion of a particle confined in a Penning trap

The highly attractive feature of Penning traps for precision measurements is that the particle motion is exactly described by the superposition of three harmonic oscillations with well-defined frequencies, assuming ideal geometry, and that the particles are stored within a small volume with energies of electron volts or below [31].

Different methods have been proposed to *decelerate* $\bar{p}$'s from LEAR energies ($\geq$ 5 MeV) to energies where antiprotons can be captured (2 – 20 keV). The simplest method is to use a degrader and to optimize its thickness to obtain a maximum number of $\bar{p}$'s in the low energy range. First results of tests done by experiment P83 indicate that a fraction 10^{-5} of antiprotons with initial energy 20 MeV leave a degrader with optimized thickness with energies below 3 keV [32]. Together with an ultrafast ejection of 10^8 $\bar{p}$ within 200 nsec from LEAR, which has been successfully tested, this can give up to 10^3 trapped antiprotons.

This method is not appropriate for experiments needing 10^6 – 10^7 stored $\bar{p}$'s, so a different post-deceleration scheme based on a radio frequency quadrupole (RFQ) decelerator [33] is under study both at CERN and at Los Alamos. This post- deceleration scheme would be also profitable for experiment P52, requiring injection energies about 100 keV.

The *dynamical trapping* of ions with 1 keV kinetic energy into a Penning trap has been demonstrated successfully at CERN [34], and tests with antiprotons are currently going on. The principle is to decelerate the incoming $\bar{p}$ bunch electrostatically, to let it enter the trap, and then to raise the Penning trap voltage to the nominal value (e.g. to 3 kV within 10 nsec) before the particles are reflected out of the confining region.

The *cooling of antiprotons* inside a Penning trap will probably require new techniques. The energy has to be brought down from the kilo- to the milli-eV region, i.e. by 6 orders of magnitude!
The routine method to cool the axial motion of particles is its damping via an external resonance circuit with high Q which is tuned precisely to the axial resonance frequency of the particle [35]. This method works fine with electrons or positrons, since the small amplitude of their motion only results in negligible frequency shifts due to anharmonicities of the harmonic potential. Unfortunately, trapped antiprotons will have large oscillation amplitudes in the initial phase, therefore the external damping circuit is only in resonance with few $\bar{p}$'s, and the cooling is inefficient.

Electron cooling inside the trap [36] might be a possible remedy. A large number of electrons, produced by ionization of background gas atoms, are stored in the same trap and cooled resistively in the standard way. The antiprotons, moving back and forth through the electron cloud, are slowed down by frictional Coulomb forces and eventually reach thermal equilibrium with the cold electrons.

Another important aspect is the *lifetime of stored $\bar{p}$'s* in the trap in the presence of background gas. The annihilation cross section increases strongly at low $\bar{p}$ energies; Fig. 8 shows the relation between average kinetic energy and annihilation rate. The storage of antiprotons with $< E > = 1$ meV needs pressures of less than 10^{-14} Torr to have lifetimes of the order of 1 day. Pressures of this order of magnitude have been reached by immersing the trap into a liquid helium bath [37].

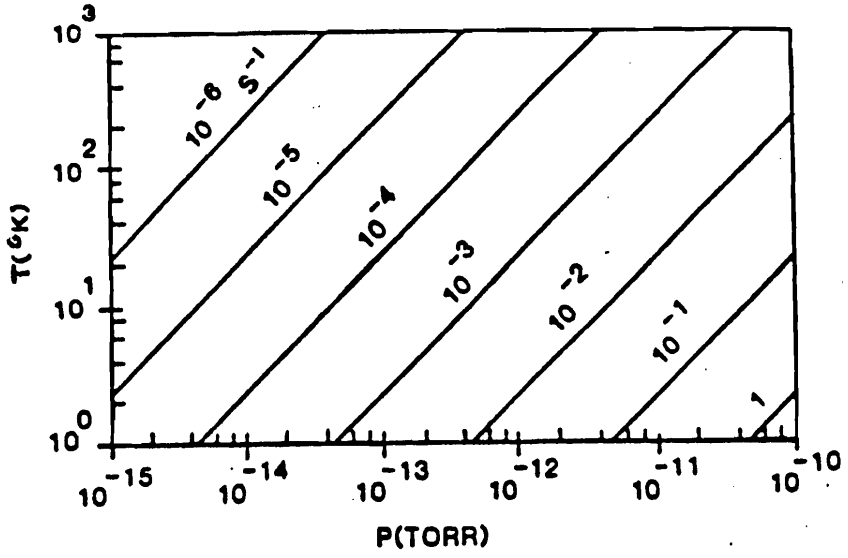

Fig. 8 Relation between rest gas pressure and annihilation rate of $\bar{p}$'s at different equilibrium temperatures in the Penning trap

2.3.2 $\bar{p}$ Inertial Mass

2.3.2.1 Penning Trap (P83)

Experiment P83 wants to measure the inertial $\bar{p}$ mass with a relative accuracy of 10^{-9} using the Penning trap technique. Only few antiprotons will be needed for the measurement, and they will be trapped, stored and cooled according to the scheme described above. Finally, 1 − 10 antiprotons will be transferred to a precision trap to determine the cyclotron frequency within a 6 T magnetic field from a superconducting magnet.

The principle of the measurement of the cyclotron frequency is: the resonant excitation of the cyclotron motion of the antiproton will reflect by an increase of the axial amplitude, since the axial and the cyclotron motion of the antiproton are coupled. The axial frequency of the $\bar{p}$ is derived from the signal induced on the endcap electrodes. An increased amplitude of the axial motion results in a small change of the axial oscillation frequency, which is compensated by a corresponding change in the endcap electrode voltage. This compensation voltage is measured while scanning many times over the cyclotron frequency region. A natural linewidth of few 10^{-9} ν_c has been achieved with this method using protons (Fig. 9) [38]. The linewidth is mainly determined by the measurement time, which can be several month. The inhomogeneity of the magnetic field is very small over the volume occupied by the stored particle (typically a few microns), and relativistic effects are negligible for particle energies in the milli−eV range.

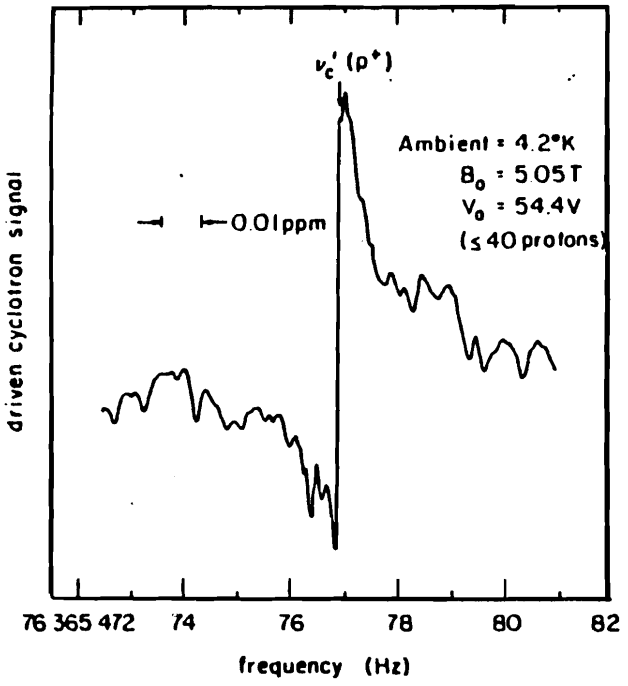

Fig. 9 Proton cyclotron resonance line (from ref. 38)

2.3.2.2 RF Spectrometer (P52)

Experiment P52 proposes a comparison of $\bar{p}$ and H^- ion masses to a precision of 10^{-9} in a RF mass spectrometer [39]. The principle of the experiment is:
$\bar{p}$ or H^- ions enter a homogeneous magnetic field through a narrow entrance slit (0.2 mm) with energies about 100 keV and rotate twice with the cyclotron frequency ν_c, following a helicoidal path inside a ring of 1 m diameter. Fig. 10 shows the scheme of the apparatus and the path of the particles.
At the end of the first and the third half−turn the kinetic energy is modulated with a frequency $\nu_m \gg \nu_c$, changing the radius R of their motion, but leaving ν_c unchanged. After the second turn, a narrow exit slit (0.2 mm) selects particles for which the sum of the two modulations is zero. This is the case if the modulation frequency ν_m is tuned to have the two modulations opposite in phase. This occurs when

$$\nu_m = (n + 1/2)\ \nu_c$$

The cyclotron frequency can thus be obtained by scanning the modulation frequency and measuring the number of particles passing through the exit slit.
The natural line width will be $10^{-6} \cdot \nu_c$ due to inhomogeneities of the magnet over spatial dimensions of 1 m, several apparative effects and the relativistic mass increase. The centroid of the peak has therefore to be determined with an accuracy of 10^{-3} relative to its width to achieve a precision of 10^{-9}.

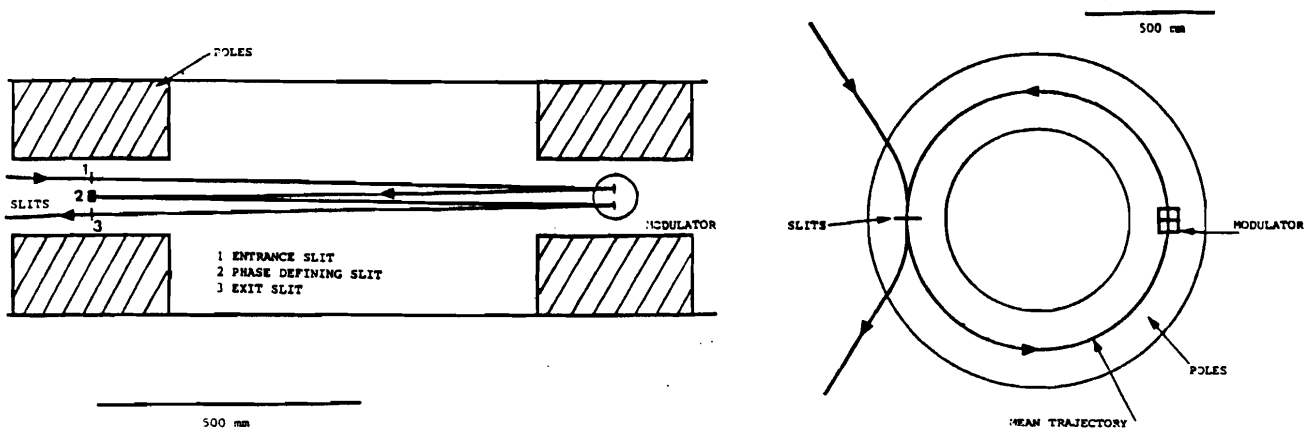

Fig. 10 Scheme of the RF mass spectrometer and the path of the particles (horizontal and vertical view)

2.3.3 Gravitational mass of the $\bar{p}$ (P94)

The schematic layout of the experiment including the deceleration and the trapping phase is shown in Fig. 11. Antiprotons will be launched from a Penning trap and ascend in a vertical drift tube of 1 m length situated in a magnetic field (6 T) guiding the path of the particles. The gravitational attraction prolongs the time of flight, and an initial kinetic energy of 10^{-7} eV is needed to overcome the 1 m height difference, assuming equal gravitational masses of proton and antiproton. A $\bar{p}$ with the minimum energy to enable it to reach the micro channel plate (MCP) detector at the end of the drift tube will arrive after 451 milliseconds. Particles arriving at these late times have started with extremely low kinetic energies and are most sensitive to gravitational effects. An accurate comparison of the tail of the drift time distribution of H^- ions and antiprotons will give the relative gravitational acceleration of the $\bar{p}$ with an accuracy of 1 %. Fig. 12 shows the expected TOF distributions for different thermal equilibrium distributions of the antiprotons in the Penning trap.

The particular difficulties of this experiment, apart from the development of a cold $\bar{p}$ source, arise from the extreme weakness of the gravitational interaction. Problems originate from stray electric fields over 10^{-7} V/m, generated e.g. by isolated charges in the drift tube, at boundaries of crystal layers ("patch effect"), or by neighbouring $\bar{p}$'s drifting in the same direction.

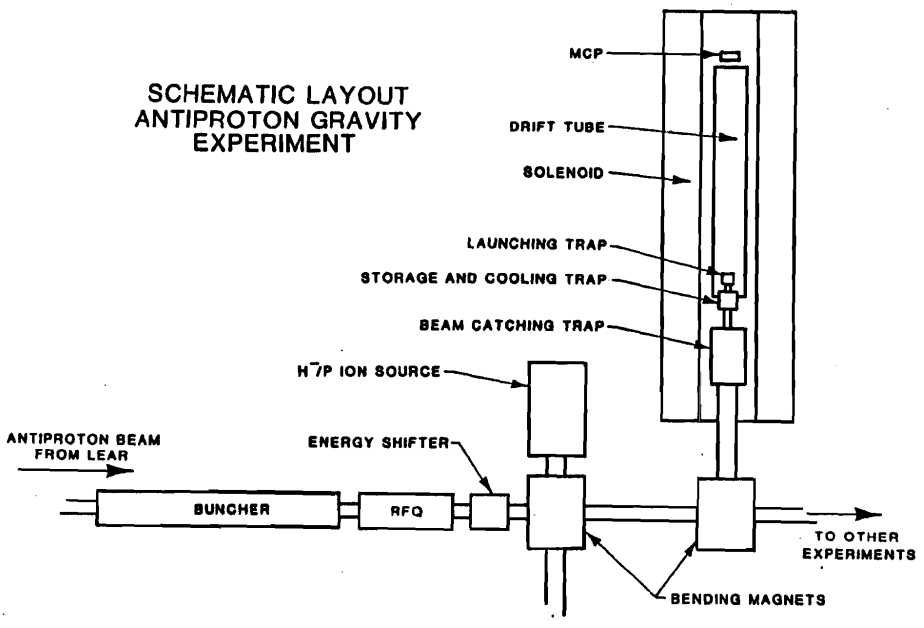

Fig. 11 Schematic layout of the antiproton gravity experiment

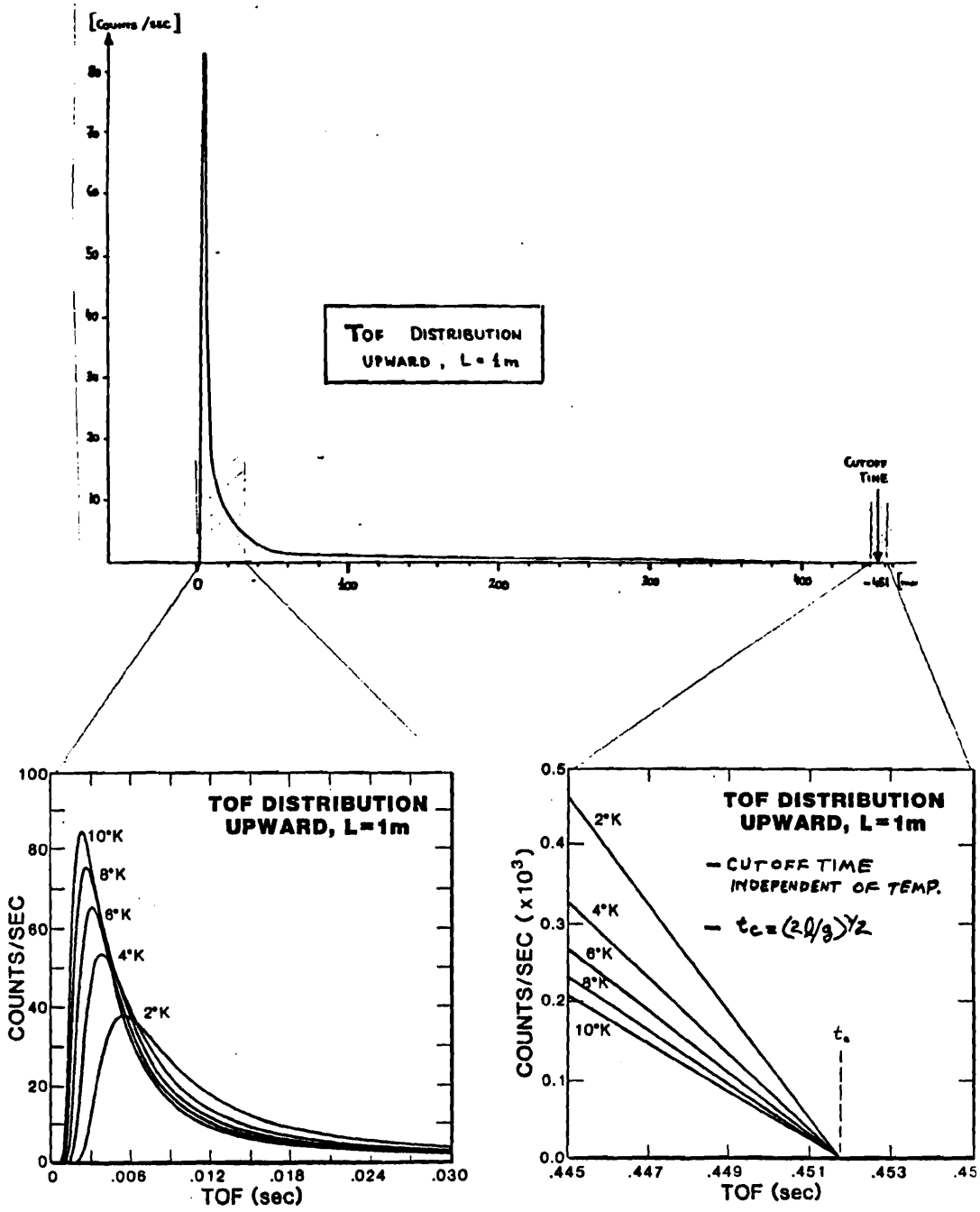

Fig. 12 Expected TOF distributions for different $\bar{p}$ equilibrium temperatures. The lower boxes contain an enlarged view of the start and end regions of the TOF distributions.

CONCLUSION

The physics programme proposed at LEAR for the post−ACOL phase after 1987 can give answers to many fundamental, but still unsolved questions of elementary particle physics at low energies: What is the origin of CP violation? Is T − or even CPT − violated? Are there "exotic" bound states of quarks and gluons? What is the dynamics of QCD confinement? What is the spin−dependence of the long range $\bar{N}N$ force? Are there macroscopic manifestations of quantum gravity?

The high data rate and the ambitious goals pursued by the experiments imply the application of state of the art techniques in the design of detectors, electronics and data acquisition. Unexpected applications of new techniques like cold $\bar{p}$ sources or polarized $\bar{p}$ beams may result from their successful demonstration at LEAR.

The future physics programme at LEAR is therefore an important source of information complementing the knowledge obtained by experiments done at the highest available energies.

Acknowledgements

This work was supported by the Deutsches Bundesministerium für Forschung and Technologie.

Proposal	Exp.	Title	Collaboration	Spokesman
P52	PS 189	High precision measurement of the $\bar{p}p$ mass difference with a RF mass spectrometer	Orsay – CERN	C.Thibault
P82	PS 195	Tests of CP violation with K^0 and $\bar{K}^0$ at LEAR	Basel – CERN – Saclay – Athens – Zurich – Fribourg – Liverpool – SIN – Stockholm – Thessaloniki	P. Pavlopoulos
P83	PS 196	Precision comparison of $\bar{p}$ and p masses in a Penning trap	Washington – Mainz – Fermilab	G. Gabrielse
P86		Feasibility Study for Antihydrogen Production at LEAR	CERN – Heidelberg – Karlsruhe	H. Poth
P90	PS 197	The Crystal Barrel: Meson Spectroscopy at LEAR with a 4π Neutral and Charged Detector	Karlsruhe – Zurich – Berkeley – Penn State – London – Surrey – Irvine – Mainz – Strasbourg – Wien – Munich	H. Koch
P91	PS 198	Measurement of Spin – Dependent Observables in the $\bar{p}N$ Elastic Scattering from 300 MeV/c to 700 MeV/c	Saclay – Karlsruhe – Lyon – SIN	R. Bertini
P92		Measurement of Spin – Dependence in $\bar{p}p$ Inter – action at Low Momenta	Heidelberg – Houston – Karlsruhe – Madison – Marburg – Mainz – Munich – Piscataway	
P93	PS 199	Study of the Spin – Structure of the $\bar{p}p \rightarrow \bar{n}n$ Channel at LEAR	Cagliari – Geneva – Karlsruhe – Trieste – Turin	F. Bradamante
P94	PS 200	Measurement of the gravitational acceleration of the antiproton	Pisa – Los Alamos – Houston – Texas A&M – Genova – Kent State – Case Western – CERN – NASA	
P95		Study of Antinucleon Annihilation at LEAR with OBELIX, a large acceptance and high resolution detector, based on the Open Axial Field Spectrometer	Brescia – Cagliari – CERN – Frascati – Geneva – Dubna – Legnaro – Orsay – Padua – Pavia – Trieste – Turin – Udine – Vancouver	U. Gastaldi
P97		JETSET: Physics at LEAR with an Internal Gas Jet Target and an Advanced General Purpose Detector	Annecy – CERN – Freiburg – Geneva – Genova – Julich – Oslo – Uppsala – Triest – Austin – Minneapolis	J. Kirkby

Table 1. Post – ACOL LEAR Proposals approved by the PSC Committee (June 1986)

Experiment	Title (abbrev.)	Location	Installation	Data taking	Total beam request [1 unit = $2 \cdot 10^{11}$ $\bar{p}$]
P52 (PS 189)	CPT: $\bar{p}$ inertial mass (RF Spectrometer)	South Hall	1988	1989	≤1
P82 (PS 195)	CP and T Violation	South Hall	1986/1987	1988 – 1992	100
P83 (PS 196)	CPT: $\bar{p}$ inertial mass	South Hall	1987	1988 – 1990	≤1
P86	CPT: $\bar{H}$ production	LEAR: SL2	3/87 – 6/87	7/87 – 12/87	7 days (dedic.)
P90 (PS 197)	$\bar{N}N$ annihilation (Crystal Barrel)	South Hall	1988	1989 – 1992	5
P91 (PS 198)	Spin: $\bar{p}N$ elastic scattering (SPESII)	South Hall	1/87 – 6/87	7/87 – 12/87	2
P92	Spin: polarized $\bar{p}$ beam (Internal Storage Cell)	LEAR: SL2	1989**		
P93 (PS 199)	Spin: $\bar{p}p \rightarrow \bar{n}n$	South Hall	1989	1990	6
P94 (PS 200)	CPT: $\bar{p}$ gravit. mass	South Hall	1990**		≤1
P95	$\bar{N}N$ annihilation (OBELIX)	South Hall	1987 – 1988	1989 – 1992	5 ($\bar{p}$) 15 ($\bar{n}$)
P97	$\bar{N}N$ annihilation (JETSET)	LEAR: SL2	1/88 – 6/88	7/88 – 12/88	12 days (dedic.)

* Approximate values. Requests rely on different assumptions on beam intensities and transfer efficiencies. Experiments inside LEAR need dedicated operation not compatible with extracted beam experiments.

** Installation at LEAR only in case of successful demonstration of the experimental technique

Table 2. Location, installation and beam time requests of post – ACOL LEAR experiments.

CP – Violation Parameters	Present Precision	10^{13} $\bar{p}$ [CP at LEAR]
$\lvert\phi_{+-} - \phi_{oo}\rvert$	5^0	2^0
$\lvert\varepsilon'/\varepsilon\rvert$	$7 \cdot 10^{-3}$	$2 \cdot 10^{-3}$
$\Delta m\ (K_S - K_L)$	$4.1 \cdot 10^{-3}$	$1.2 \cdot 10^{-3}$
$\lvert\eta_{+-o}\rvert$	$< 1.2 \cdot 10^{-1}$	$< 6 \cdot 10^{-4}$
$\lvert\eta_{ooo}\rvert$	$< 10^{-1}$	$< 8 \cdot 10^{-4}$
Re X	$< 2 \cdot 10^{-2}$	$< 6 \cdot 10^{-4}$
Im X	$< 2.6 \cdot 10^{-2}$	$< 7 \cdot 10^{-4}$
A_T	–	$6.4 \cdot 10^{-2}$

Table 3. Comparison of present and achievable precision of CP and T violation parameters

	Bubble Ch.	ASTERIX	Crystal Barrel*	OBELIX
Events	10^5	10^7	$2 \cdot 10^7$	$2 \cdot 10^7$
Charged tracks				
Acceptance:				
moment. meas.	100 %	60 %	63 %	75 %
tracking	100 %	85 %	100 %	100 %
Mom. resol. σ [1 GeV/c]	3 %	5.5 %	2.8 %	2.7 %
π/K separation	< 450 MeV/c	< 400 MeV/c	< 500 MeV/c	< 1000 MeV/c
Gamma detection				
Acceptance	–	25 %	80 %	80 %
Angular resol. σ	–	150 mrad	30 mrad	2 mrad
Energy resol. σ [1 GeV]	–	–	2 %	18 % (2.5 % pair spectr.)
Trigger				
Charged track mult.	–	Yes	Yes	Yes
Gamma multiplicity	–	Yes	Yes	Yes
$\gamma\gamma$ invariant mass	–	–	Yes	–
K_S	–	Yes	Yes	Yes
Charged kaon	–	–	–	Yes

* Design values

Table 4. Comparison of the main parameters of previous and proposed detectors to study $\bar{N}N$ annihilation

REFERENCES

[1] K. Kilian, "Results from LEAR", these proceedings
A comprehensive presentation of the first LEAR results is contained in: Proceedings of the 3rd LEAR Workshop on Physics with Antiprotons at LEAR in the ACOL Era, Tignes 1985; eds. U. Gastaldi, R. Klapisch, J.M. Richard and J. Tran Thanh Van; (Editions Frontières, Gif-sur-Yvette, 1985)

[2] D. Hertzog et al., Investigation of the $\bar{p}p \to \xi(2220) \to K_S K_S$ reaction at LEAR, Proc. 3rd LEAR Workshop, Tignes 1985, p. 403

[3] J. Duclos et al., Status and Future of the experiment PS 170, Proc. 3rd LEAR Workshop, Tignes 1985, p. 517

[4] L. Wolfenstein, Present Status of CP Violation, February 1986; to be published in: Ann. Rev. of Nucl. and Part. Science; and references therein

[5] E. Gabathuler and P. Pavlopoulos, in: Proc. 2nd Workshop on Physics at LEAR with Low Energy Cooled Antiprotons, Erice 1982; eds. U. Gastaldi and R. Klapisch (Plenum Press, New York, 1984) p. 747

[6] "Review of Particle Properties", Rev. of Mod. Physics, Vol. 56, No. 2, Part II; April 1984

[7] P.K. Kabir, Phys. Rev. D2 (1970) 540

[8] M. Chanowitz, Proc. Summer Inst. on Particle Physics, Stanford 1981; ed. A. Mosher (SLAC, Stanford, 1982) p. 41

[9] C. Dover, Nucl. Phys. A416 (1984) 313

[10] C. Dover, Proc. Int. Symposium on Medium Energy Nucleon and Antinucleon Scattering, Bad Honnef (Germany), 1985, and BNL 36821; and references therein

[11] J. Bystricky, F. Lehar, and P. Winternitz, J. Physique 39 (1978) 1

[12] C. Beard et al., Phys. Lett. B155 (1985) 437

[13] C. Dover, Low Energy $\bar{p}p$ Interaction: Theoretical Perspective, Proc. of the Workshop on the Design of a Low Energy Antimatter Facility in the USA; Madison, Wisconsin, 1985

[14] Y. Onel, these proceedings

[15] see, for example: C.B. Dover and J.M. Richard, Phys. Rev. C21 (1980) 1466
J.M. Richard, Proc. 2nd LEAR Workshop on Physics at LEAR, Erice 1982; eds. U. Gastaldi and R. Klapisch (Plenum Press, New York, 1984) p. 447 and references therein

[16] P. Fayet, Phys. Lett. 95B (1980) 285

[17] J. Scherk, in: Unification of the Fundamental Particle Interactions, eds. S. Ferrara, J. Ellis and P. van Nieuwenhuizen (Plenum Press, New York, 1981)

[18] G. W. Gibbons and B.F. Whiting, Nature 291 (1981) 636
P. Hut, Phys. Lett. 99B (1981) 174
K.I. Macrae and R.J. Riegert, Nucl. Phys. B244 (1984) 513
Y.T. Chen et al., Proc. Roy. Soc. (London) A394 (1984) 47
V.K. Milyukov, Sov. Phys. JETP 61 (1985) 187

[19] S.C. Holding and G.J. Tuck, Nature 307 (1984) 714
F.D. Stacey et al., Phys. Rev. D23 (1981) 1683

[20] R. Neumann et al., Z. Phys. A313 (1983) 253

[21] B. Deutch, these proceedings

[22] U. Gastaldi et al., Nucl. Instr. Methods 157 (1978) 441

[23] O. Botner et al., Nucl. Instr. Methods 196 (1982) 315

[24] U. Gastaldi, Nucl. Instr. Methods 188 (1981) 459
[25] M.P. Bussa et al., High Density Spiral Projection Chamber, CERN – EP/86 – 49, Contrib. to the Vienna Wire Chamber Conference 1986
[26] C. Baglin et al., CERN – EP/85 – 01
[27] I.F. Silvera et al., Phys. Rev. Lett. 37 (1976) 136
[28] J. Séguinot et al., Invited Paper presented at the Vienna Wire Chamber Conference 1986
[29] C.J.S. Damerell, Proc. 12th SLAC Summer Institute on Particle Physics (1984) p. 43
[30] D. Rust (HRS Collab.), Invited Paper presented at the 3rd Int. Conf. on Instrumentation for Colliding Beam Physics, Novosibirsk, USSR (1984), SLAC – PUB – 3311
D. Ribon et al. (MAC Collab.), Proc. 12th SLAC Summer Institute on Particle Physics (1984) p. 332
[31] L.S. Brown and G. Gabrielse, to be published in: Review of Modern Physics
[32] H. Kalinowsky, private communication
[33] R.H. Stokes, T.P. Wangler, and K.R. Crandall, 1981 Particle Accelerator Conference, Washington, D.C.
T.P. Wangler, K.R. Crandall, and R.H. Stokes, Symp. on Accel. Aspects of Heavy – Ion Fusion, GSI, Darmstadt (1982)
C. Biscarri and F. Iazzourene, Post – Deceleration of the LEAR beam by a RFQ, Proc. 3rd LEAR Workshop, Tignes
[34] H. Schnatz et al., In – Flight Capture of Ions into a Penning Trap, CERN – EP/86 – 43, April 1986; submitted to Nucl. Instr. and Methods
[35] P.B. Schwinberg, R.S. Van Dyck, and H.G. Dehmelt, Phys. Lett. 81A (1981) 119
[36] W. Kells, G. Gabrielse, and K. Helmerson, Fermilab – Conf. – 84/68 – E, originially presented at the ICAP IX meeting in Seattle, Wa. in August 1984
[37] W. Thompson and S. Hanrahan, J. Vac. Sci. Tech. 14 (1977) 643
[38] R.S. Van Dyck and P.B. Schwinberg, Phys. Rev. Lett. 47 (1981) 395
[39] L.G. Smith and A.H. Wapstra, Phys. Rev. C11 (1975) 1392